Forces in Mechanics 3 (2021) 100017

Contents lists available at ScienceDirect

Forces in Mechanics

journal homepage: www.elsevier.com/locate/finmec

Numerical model development to predict the process-induced residual stresses in fibre metal laminates

Costanzo Bellini*, Vittorio Di Cocco, Francesco Iacoviello, Luca Sorrentino

Department of Civil and Mechanical Engineering, University of Cassino and Southern Lazio, via G.Di Biasio 43, 03043 Cassino, Italy

ARTICLE INFO

Keywords:
Fibre metal laminate
Cure induced deformation
Residual stresses
Finite element analysis

ABSTRACT

The thermomechanical interactions between the different materials constituting a hybrid laminate make residual stresses arise during the manufacturing process of such laminate. In turn, the residual stresses make the laminate deform as it is extracted from the mould. Cure induced deformation represent a problem for the assembly step, since additional operations are required for allowing the joining of the different components. Therefore, a tool suitable for the calculation of residual stresses and deformation is needed in order to predict them and to implement the necessary remedies. In the present work, a numerical model for the determination of residual stresses is presented and validated through experimental tests. The case study was a notched laminate, in order to emphasize the deformation without altering the thermal cycle experienced in the material. Both numerical and experimental runs highlighted a higher deformation near the vertex of the laminate.

1. Introduction

FMLs (Fibre metal laminates) are a class of hybrid materials constituted by metal sheets alternate to composite material laminate. FMLs present interesting mechanical properties, due to the combination of the constituent materials; in fact, they have higher damage tolerance and after-impact residual strength than metals or composites, coupled to higher fatigue life and both strength-to-weight and stiffness-to-weight ratios [1,2]. For this reason, FMLs are more and more used to produce aircraft parts, like the Airbus A380 fuselage, that are made of GLARE, an FML made of aluminium sheets and glass fibre composite. However, the FMLs suffer process-induced defects, that consist in residual stresses development and the consequent laminate deformation, that give rise to issue during the assemblage of the parts. The residual stresses are caused by different phenomena that happen during the curing process of the composite material. There are different sources for the residual stresses, and they can be categorized into two groups: thermoelastic and non-thermoelastic. The former ones are those that can be recovered by heating the part. They spring out during the cooling, after the curing process, and are caused by the mismatch between the CTEs (coefficient of thermal expansion) of the metal and the composite material, being the former one higher than the latter one. During the heating ramp of the curing process, the resin of the composite material is in the liquid state and it is not able to bear loads; therefore, there is the reciprocal shifting of the material layers, till the resin vitrification, that happens at high temperature. In such an instant, the resin becomes a solid and all the layers are glued together; consequently, any reciprocal movement is blocked. During the cooldown, the metal layer shrinkage is larger than the composite layer one, but the material continuity must be maintained, so residual stresses are generated. The non-thermoelastic stresses are due to phenomena that happen before cooldown and they cannot be recovered by heating the laminate. Two factors belong to this group: the resin chemical shrinkage and the part-tool interaction. The polymer crosslinking makes the resin specific volume decrease, giving rise to an effect similar to the CTE one, but it cannot be recovered by heating the part since the resin polymerization is an irreversible event [3]. The latter residual stresses source, the tool-part interaction, is caused by the action of the mould on the laminate [4]. In fact, the CTE of the mould material is higher than that of the laminate, so the mould pulls the laminate during the heating up. This happens when the resin is still liquid, so the layers closer to the mould are more stretched than the other ones, and this stress distribution remains frozen in the material as the resin cures, giving rise to unbalanced residual stresses after demoulding.

Process induced residual stresses and distortion have been deeply investigated for the composite materials, while few works are relevant to FMLs distortions. Abouhamzeh et al. [5] proposed a numerical model for the prediction of cure induced distortion of FML, that can be used to improve the design of parts made with this material. They separated the thermoelastic phenomena from the non-thermoelastic ones by reheating cured laminates and evaluating the residual deformation. The same authors presented a new numerical procedure to evaluate the residual stresses in material experiencing small strains and large rotations, considering temperature-dependent mechanical properties for the material. The model accuracy was determined by comparing numerical results with experimental ones [6]. Guangquan et al. [7] developed a model to simulate the residual stress development in FMLs, studying both a

* Corresponding author.
E-mail address: costanzo.bellini@unicas.it (C. Bellini).

https://doi.org/10.1016/j.finmec.2021.100017
Received 15 February 2021; Received in revised form 19 March 2021; Accepted 20 March 2021
Available online 26 March 2021

plane laminate and an L-shaped one. Kappel et al. [8] proposed an experimental methodology to determine the stress-free temperature, that indicates the instant when the metal sheets become joined with the composite material layers. The presented solution was based on both strain gages and fibre Bragg sensors, that were used for evaluating the strains in both constituent materials. Tinkloh et al. [9] proposed a numerical homogenization technique to calculate the deformation of a hybrid metal-composite plate: the heterogeneous microstructure of the hybrid plate was homogenized by using a specific scheme, allowing the passing from the microscale to the macroscale. The proposed technique was validated by comparison with experimental tests. Hanson et al. [10] suggested a simplified method for calculating the residual stresses of composite material-metal parts, that took into consideration the resin cure shrinkage and the difference in CTE between the constituent materials. The proposed methodology was validated by experimentally measuring the residual stresses developing in a metal-composite hybrid ring. Ding et al. [11] proposed and validated a numerical model to calculate the residual stresses in a composite material laminate, then the analysis was repeated on a laminate covered with aluminium skins, finding that the composite cure trend was not affected by them, while they influenced the development of residual stresses. Prussak et al. [12] introduced a supplementary cooling step in the cure thermal cycle of a carbon-based FML for reducing the residual stresses. Krimbalis et al. [13] proposed an analytical model for the calculation of residual stresses in FMLs, that was validated by comparing the obtained results with those determined by FEM. Bellini et al. [14] proposed FML as a solution to decrease the flange to flange angle in L-shaped laminates; in fact, they substituted the central plies of prepreg with an aluminium sheet, obtaining a reduction of the deviation angle equal to about 40%. Yuan et al. [15] presented an analytical model for the determination of both the relative movement between the metal and the composite during heating up, and the final deformation of the laminate at the end of the curing process. Che et al. [16] studied the FML deformation by using an analytical model, that was validated through numerical and experimental results.

In the present work, a numerical model for the simulation of the curing process for FMLs is presented and validated. In particular, a notched flat specimen was considered in this study; in that manner, the halves were free to move reciprocally, causing the accentuation of the part deformation, but the stacking sequence was the same as for a common FML. Therefore, the thermal cycle experienced in the material was the same too. In the past literature, similar activities had been carried out on unsymmetrical laminates, constituted by a metal sheet and a layer of composite [9]. This solution was suitable to remark the material deformation, but the thermal cycle experienced by the studied material was not the same as that of an FML. Instead, the methodology presented in this work was suitable for achieving both objectives, that are highlighting the deformations in a material that has undergone the standard thermal cycle. A FEM model suitable for the curing process simulation of composite materials was modified and adapted for the manufacturing process simulation of FMLs. The proposed model was verified by comparing the achieved results with others obtained from experimental tests.

2. Materials and methods

The reference case study considered in this article was a rectangular hybrid laminate, whose dimensions were 350 mm × 300 mm. The laminate was constituted by three EN AW 3105 aluminium alloy sheets, whose thickness was 0.8 mm, and two layers of carbon composite, each one constituted by two prepreg plies, with a thickness of 0.25 mm. The raw composite material used in this work was made of epoxy resin and AS4 carbon fibre fabric, characterized by the satin weave style. A structural film adhesive, the AF 163-2, was adopted to bond the aluminium sheets to the composite material. As it can be seen from Fig. 1, the two metal sheets were the outer surfaces of the laminate, while the third one was in the centre; the composite material layers were disposed in alternate positions with respect to the metal sheets. The notches were created in the laminate by partially substituting the adhesive with a PTFE (Polytetrafluoroethylene) film, for avoiding the sticking of the prepreg to the central metal sheet. The notches were four in number and their depth was equal to 65 mm. As abovementioned, a numerical model suitable for simulating the process-induced deformation was presented and verified: in the following paragraphs, both the numerical model and the experimental tests for its validation are described.

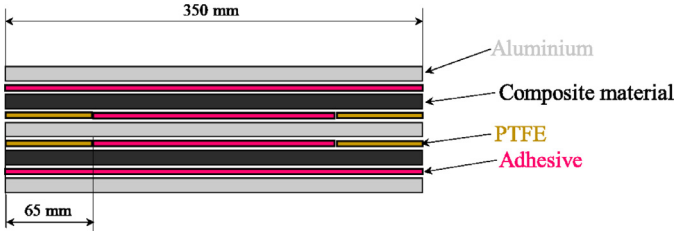

Fig. 1. stacking sequence and geometrical characteristics of the studied laminate.

2.1. Numerical model

The numerical model for the simulation of the residual stresses developed during the curing cycle derived from those usually applied for the curing process simulation of composite materials. These models take into account several aspects relevant to the resin cure, such as the chemical shrinkage and the cure kinetic, and the boundary conditions, such as the mechanical interaction with the mould, the heat flow and the vacuum bag pressure, and then they give information about temperature, degree of cure, residual stresses and, as a consequence, deformation. For the correct simulation of the curing process, some features should be considered: the fixing of the material parameters, the definition of boundary condition and the selection of the physical models.

As concerns the last one, two different types of sub-models were adopted: the resin polymerization was simulated through the thermochemical sub-model, while the residual stresses arise was calculated through the thermomechanical one. The former one depended on the heat balance [17]:

$$\rho_c c_c \frac{dT}{dt} = \nabla\left(k_c \nabla T\right) + \rho_r V_r \dot{Q} \tag{1}$$

In the Eq. (1), ρ represents the material density, c is the specific heat, T is the temperature, t is the time, k is the thermal conductivity coefficient, $\dot{Q}$ is the heat generation rate of the resin polymerization reaction, which is exothermic, and V is the volumetric percentage. The subscripts r and c refer to resin and composite material, respectively. Some properties of composite material, such as density and specific heat, were calculated from those of the constituents by considering the volumetric fraction content [18]. For calculating the heat generation rate, it should be remembered that it depends on the cure rate ($d\alpha/dt$) and the total heat of reaction H_r according to the following relation [19]:

$$\dot{Q} = \left(\frac{d\alpha}{dt}\right) H_r \tag{2}$$

where the cure rate can be determined as

$$\frac{d\alpha}{dt} = K(T) \cdot f(\alpha) \tag{3}$$

Being

$$f(\alpha) = \alpha^m (1-\alpha)^n \tag{4}$$

in which n and m represent the reaction orders. On the other hand, K(T) may be defined through an Arrhenius type relation:

$$K = A_c \exp\left(-\frac{E}{RT}\right) \tag{5}$$

where A_c is the frequency factor, E is the activation energy, and R is the universal gas constant.

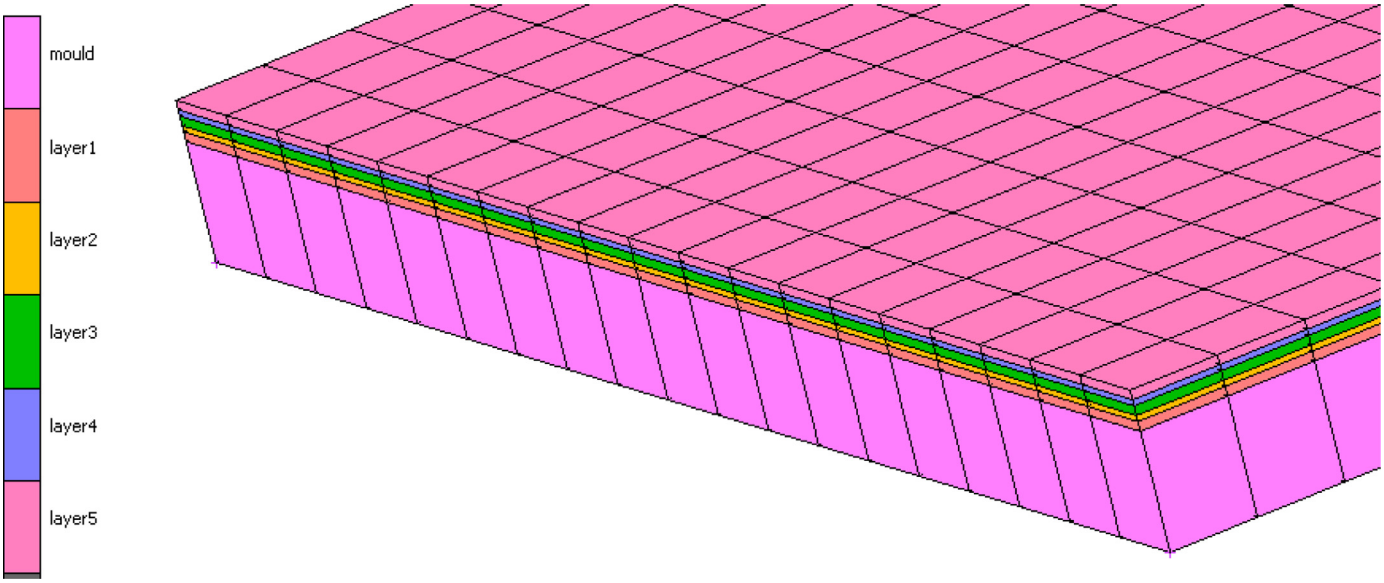

Fig. 2. calculation mesh prepared for the present study.

The thermomechanical model was coupled to the thermochemical one and described the evolution of strain ε and stresses σ in the material. The mechanical agents acting in the domain were the pressure due to the vacuum bag, the interaction with the mould, the thermal expansion, and the chemical shrinkage of the resin. For each i-th material, the thermal expansion can be simulated as

$$\varepsilon_i^T = CTE_i\left(T - T_0\right) \tag{6}$$

in which T_0 represent the stress-free temperature. The model for the resin chemical shrinkage depends on the resin volumetric cure shrinkage V_r^s as described by the subsequent equation:

$$\varepsilon_r^s = \left(1 + V_r^s\right)^{1/3} - 1 \tag{7}$$

In turn, V_r^s can be calculated from the cure degree α, according to the following equation:

$$\begin{aligned} V_r^S &= 0.0 \quad for \quad \alpha < \alpha_{C1} \\ V_r^S &= A * \alpha_S + \left(V_r^{S\infty} - A\right) * \alpha_S^2 \quad for \quad \alpha_{C1} \le \alpha \le \alpha_{C2} \\ V_r^S &= V_r^{S\infty} \quad for \quad \alpha \ge \alpha_{C2} \\ \alpha_S &= \frac{\alpha - \alpha_{C1}}{\alpha_{C2} - \alpha_{C1}} \end{aligned} \tag{8}$$

where α_{C1} stand for the cure degree level in which the resin cure shrinkage starts, while α_{C2} is that one in which the shrinkage ends, and the cure degree variation between these two values is denoted by α_s. The total resin volumetric chemical shrinkage is represented by $V_r^{s\infty}$, while the linear cure shrinkage coefficient by A. The material properties considered in this work, that are reported in Tables 1 and 2 for the composite material and the aluminium, respectively, were found in the material datasheet or determined through experimental tests.

The numerical simulation was subdivided into two steps: the first one regarded the cure cycle, with the heating of the material, the dwell at high temperature, during which non-thermoelastic residual stresses developed, and the cooldown, during which thermoelastic residual stresses grew. The second simulation step was relevant to the demoulding, that was characterized by the deformation due to the release of previously developed residual stresses. Due to the symmetry of both the domain geometry and boundary conditions, in order to reduce the necessary computational efforts, only a quarter of the laminate and the mould was simulated. The latter consisted in a 10 mm thick plate made of aluminium. Each simulation step was characterized by specific boundary conditions: for the first one, the mould was isostatically blocked in the space, allowing the free deformation due to thermal expansion and chemical shrinkage, while the pressure equal to 1 bar, representing the action of the vacuum bag, was applied on the upper and the lateral surfaces of the laminate. Moreover, a convective heat flow was considered on the exposed surfaces; the convective heat transfer coefficient was equal to 70 W/m^{2}K, while the thermal cycle consisted of a heating ramp at 145°C in one hour, a dwell of two hours at this temperature and a subsequent cool down till room temperature, reached in half an hour. A sliding contact with a friction coefficient of 0.7 was considered between the mould and the first aluminium sheet of the laminate, while a sliding contact with a friction coefficient of 0.1 was set at the

Table 1
composite material properties for numerical modelling.

Property	Value
Density [kg/m^3]	$\rho_r = 1250$; $\rho_c = 1580$
Specific heat [J/kgK]	$C_c = 950$
Thermal conductivity [W/mK]	$k_1 = k_2 = 4.65$; $k_3 = 0.45$
Activation energy [J/mol]	79856
Pre-exponential factor [s^{-1}]	1.08×10^9
m	0.89
n	0.81
Reaction heat [J/Kg]	250000
Young's moduli [Pa]	$E_{11} = E_{22} = 4\times10^{10}$; $E_{33} = 4\times10^9$
Poisson's moduli	$\nu_{12} = 0.3$; $\nu_{31} = 0.0165$; $\nu_{23} = 0.25$
Shear moduli [Pa]	$G_{12} = 2.327\times10^9$; $G_{31} = G_{23} = 1.6\times10^8$
CTE (longitudinal)	8×10^{-7}
CTE (transverse)	1.5×10^{-6}
Total volumetric cure shrinkage	0.0185
α_{C1}	0.055
α_{C2}	0.66
A coefficient	0.173

Table 2
Aluminium properties for numerical modelling.

Property	Value
Density [kg/m^3]	2700
Specific heat [J/kgK]	900
Thermal conductivity [W/mK]	117
Young's modulus [Pa]	7×10^{10}
Poisson's modulus	0.3
CTE	8×10^{-5}

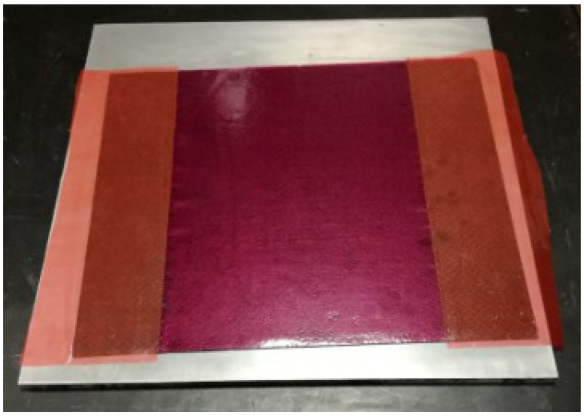

Fig. 3. laying down of the raw materials: the positioning of the short adhesive layer together with the PTFE film.

notch interface. Being the adhesive film thickness negligible compared to the thickness of the other layers, the presence of the adhesive was simulated by matching the nodes of the different layers at the interface where the adhesive was present. As concerns the demoulding step, it was simulated by isostatically blocking the laminate and moving the mould downwards, till the complete separation of the latter from the former was achieved.

The calculation domain was modelled using 8-node hexahedral elements. In particular, the mould was constituted by a single layer of elements, while for the laminate five layers were considered, one for each of the different layers of the laminate. A detail of the drawn mesh is reported in Fig. 2, where the different layers are highlighted.

2.2. Experimental tests

The proposed numerical model for the simulation of the cure-induced residual stresses was validated through comparison with results from experimental tests. A laminate identical to that one of the numerical model was produced by using the prepreg vacuum bag technology. First of all, the mould, that was an aluminium plate with dimensions of 400 mm × 400 mm × 10 mm, was covered with the release agent for allowing the removal of the laminate during the demoulding. Then, the raw materials, that are the aluminium sheets, the prepreg layers, and the adhesive film, were cut to obtain rectangular pieces with the same dimensions as the laminate. These sheets were piled following the prefixed stacking sequence; therefore, at first an aluminium sheet was placed on the mould, followed by the adhesive film and two layers of composite prepreg. In the centre of this last layer a piece of adhesive film, whose length was 220 mm, was positioned, while two pieces of PTFE film were laid down in the exterior part, in order to avoid any sticking of the composite to the central metal sheet and to generate the notches, as visible in Fig. 3, where the adhesive film is violet coloured and the PTFE film is red coloured. The lamination sequence was continued by adding the second aluminium sheet, the short adhesive film with the PTFE pieces for notch creation, the remaining composite material layers, the last adhesive film and the third aluminium sheet. The raw material stack was covered with the ancillary materials, that are the release film and the breather; then, it was sealed in the vacuum bag and it was placed in an oven for the curing process.

After the end of the curing cycle, the laminate was demoulded and the residual stresses, that developed during the curing process, were re-

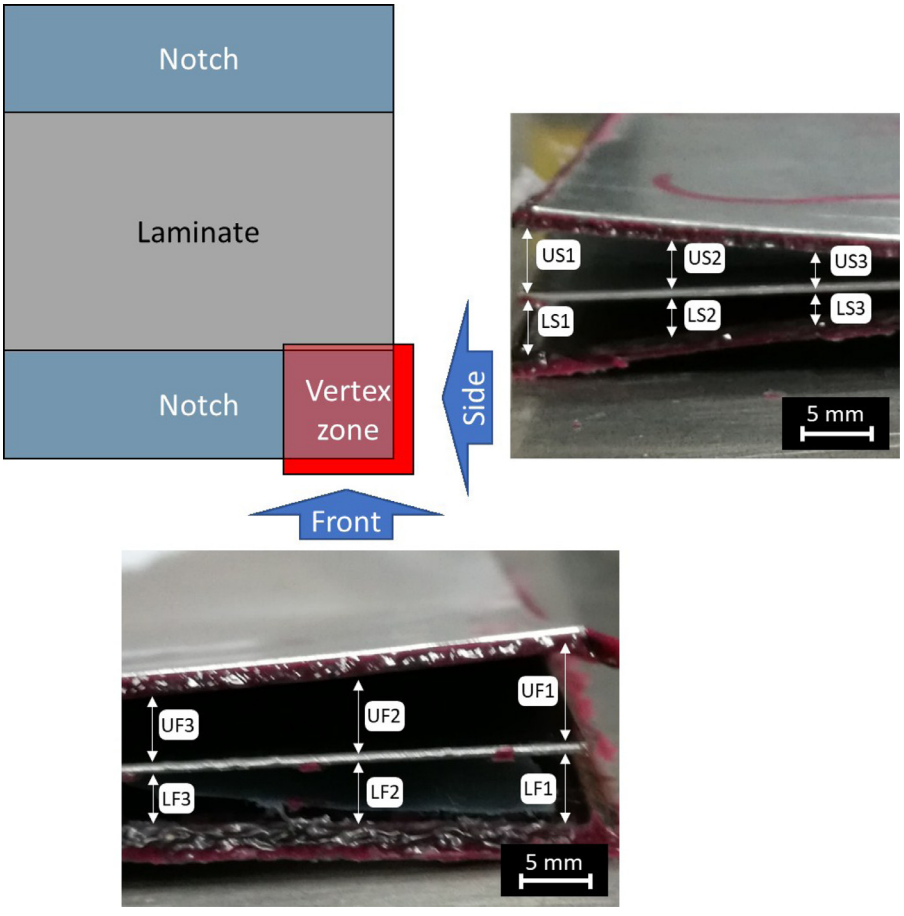

Fig. 4. measurement strategy to evaluate the notch opening.

Table 3
Notch opening obtained from experimental tests.

	UF1	UF2	UF3	LF1	LF2	LF3	US1	US2	US3	LS1	LS2	LS3
Mean value [mm]	4.42	3.88	3.02	4.44	4.20	3.56	4.47	3.15	2.08	4.49	3.42	2.22
Standard deviation	0.33	0.30	0.26	0.38	0.40	0.25	0.34	0.28	0.17	0.43	0.31	0.19
Coeff. of variation	7.57%	7.82%	8.57%	8.52%	9.62%	7.03%	7.71%	8.88%	8.17%	9.58%	9.06%	8.56%

Table 4
Comparison between experimental tests and numerical simulation results.

	UF1	UF2	UF3	LF1	LF2	LF3	US1	US2	US3	LS1	LS2	LS3
Experimental value [mm]	4.42	3.88	3.02	4.44	4.20	3.56	4.47	3.15	2.08	4.49	3.42	2.22
Numerical value [mm]	4.84	4.20	3.26	4.92	4.57	3.85	5.00	3.42	2.22	4.96	3.74	2.39
Difference from exp.	9.6%	8.3%	7.8%	10.7%	8.8%	8.0%	11.8%	8.6%	6.9%	10.5%	9.3%	7.7%

leased, generating the deformation of the laminate. The deformed laminate presented an opening of the notch, especially near the vertex. For evaluating the laminate distortion, a contactless methodology, based on image analysis, was implemented. In particular, a total of 12 measurements were carried out near each vertex: as visible in Fig. 4, three points were considered for the side view of the upper notch (US1, US2 and US3) and three for the lower one (LS1, LS2 and LS3), and the same for the front view, that is UF1, UF2 and UF3 for the upper notch and LF1, LF2 and LF3 for the lower notch.

3. Results

The results obtained in this research work are reported in this section. First of all, the measurement data acquired in the experimental campaign are described; then, the outcomes of the numerical simulation are illustrated and a comparison with the experimental ones is carried out to validate the proposed model.

The measures of the notch opening evaluated in the experimental tests are reported in Table 3. In this table, the measurement of each of the aforementioned points is averaged over all the three manufactured laminates and the four vertexes of each laminate. This last operation was performed since the laminates were bisymmetric. Therefore, the value reported for each point is the average over 12 measurements. Moreover, the standard deviation and the coefficient of variation, that is the ratio between the standard deviation and the average value of measurements [20], are reported in the same table. The achieved experimental results showed that the maximum deformation was obtained at the tip of the vertex; in fact, the notch opening was almost 4.5 mm. On the contrary, the minimum value was found for the furthest point from the tip, and it was about 3.3 mm for the front view and 2 mm for the side view. Obviously, no significative difference was observed between the two different views for point 1 since they were very close to each other, while an increasing difference was noted for points 2 and 3 since they are more distant from each other.

The results reached through the experimental tests were used for validating the numerical model proposed in this work. In particular, a simulation was carried out and the notch opening was evaluated at different points by using the software measuring tool. The results of the numerical run are showed in Table 4, where the experimental ones are reported together with the comparison with the former ones. It can be noted that the numerical model tended to overestimate the deformation; in fact, a positive difference was found for all the considered points. However, the overestimation was acceptable since it was slightly over 10% only in a few cases. Moreover, it can be noted that the deviation is higher for the point closest to the vertex tip, and it is lower for the farthest.

A contour map of the laminate deformation is reported in Fig. 5. It can be seen that the zone near the vertex tip is the most deformed, as de-

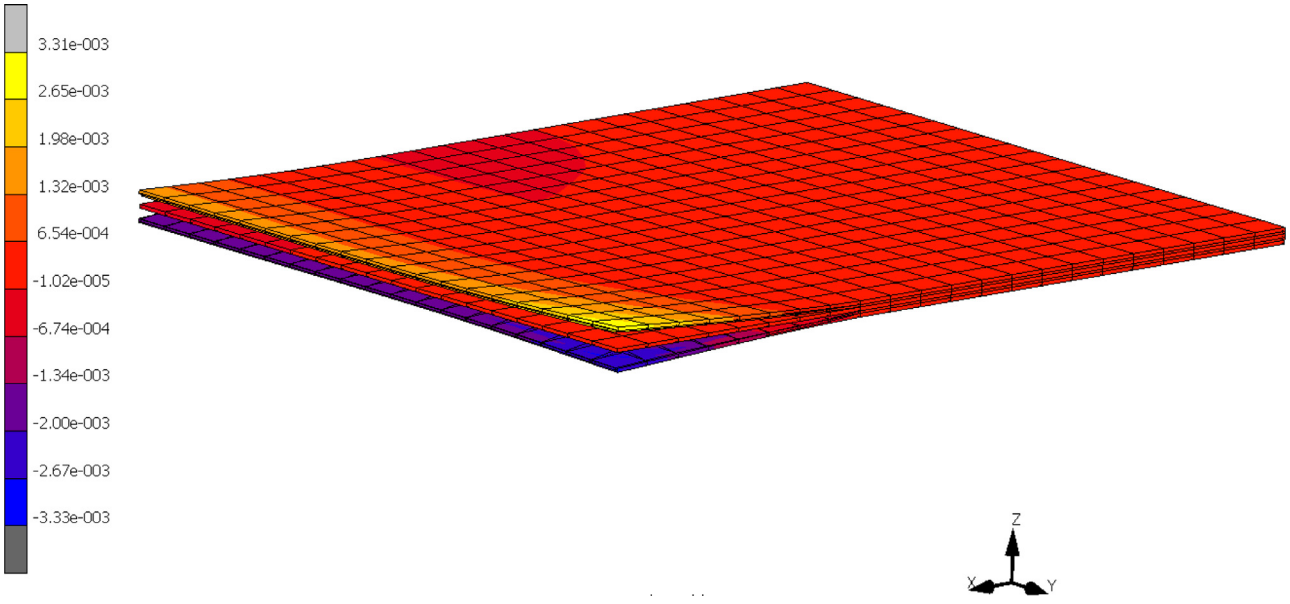

Fig. 5. z-displacement [m] evaluated by numerical simulation.

noted by the yellow area on the upper surface and the violet one on the lower surface, in the neighbourhood of the tip, while the deformation in the central zone is lower.

4. Conclusions

In the present work, a numerical model for the simulation of cure-induced deformations in FML (fibre metal laminates) materials was introduced and validated. The numerical model derived from those suitable for the simulation of the curing process of composite materials. It was composed of two sub-models: the thermochemical one, for accounting of the chemical transformations, happening in the matrix of the composite layers, and the thermomechanical one, that was needed for describing the mechanical interactions between the different materials constituting the FML.

The numerical model was validated by comparing the displacement evaluated on the deformed mesh with those measured in some produced specimens. The laminates manufactured in this work presented some notches: in that manner, the part deformation was emphasized, but the stacking sequence was the same as for a common FML, in order not to alter the thermal cycle experienced in the material. The comparison activity carried out between the numerical and the experimental results demonstrated the strength of the model and its suitability for the determination of the process-induced deformation in FMLs. In fact, the deviation achieved between experimental and numerical results was reasonable, since it was about 10%. Moreover, both the experimental test and the numerical model evidenced that the highest deformation was located near the vertex tip of the laminates, where the notch opening was more than 4 mm.

Declaration of Competing Interest

The authors declare that they have no known competing financial interests or personal relationships that could have appeared to influence the work reported in this paper.

References

[1] C. Bellini, V. Di Cocco, F. Iacoviello, L. Sorrentino, Experimental analysis of aluminium carbon/epoxy hybrid laminates under flexural load, Frat. Ed Integr. Strutt. 49 (2019) 739–747, doi:10.3221/IGF-ESIS.49.66.

[2] C. Bellini, V. Di Cocco, L. Sorrentino, Interlaminar shear strength study on CFRP/Al hybrid laminates with different properties, Frat. Ed Integr. Strutt. 51 (2020) 442–448, doi:10.3221/IGF-ESIS.51.32.

[3] I. Baran, K. Cinar, N. Ersoy, R. Akkerman, J.H. Hattel, A review on the mechanical modeling of composite manufacturing processes, Arch. Comput. Methods Eng. 24 (2017) 365–395, doi:10.1007/s11831-016-9167-2.

[4] E. Kappel, Forced-interaction and spring-in – relevant initiators of process-induced distortions in composite manufacturing, Compos. Struct. 140 (2016) 217–229, doi:10.1016/j.compstruct.2016.01.016.

[5] M. Abouhamzeh, J. Sinke, R. Benedictus, Investigation of curing effects on distortion of fibre metal laminates, Compos. Struct. 122 (2015) 546–552, doi:10.1016/j.compstruct.2014.12.019.

[6] M. Abouhamzeh, J. Sinke, R. Benedictus, A large displacement orthotropic viscoelastic model for manufacturing-induced distortions in fibre metal laminates, Compos. Struct. 209 (2019) 1035–1041, doi:10.1016/j.compstruct.2017.06.009.

[7] Y. Guangquan, Z. Jiazhen, M. Songhe, Study on cure-induced residual stresses for fibre metal laminate, Polym. Polym. Compos. 21 (2013) 561–564, doi:10.1177/096739111302100902.

[8] E. Kappel, R. Prussak, J. Wiedemann, On a simultaneous use of fiber-Bragg-gratings and strain-gages to determine the stress-free temperature Tsf during GLARE manufacturing, Compos. Struct. 227 (2019) 111279, doi:10.1016/j.compstruct.2019.111279.

[9] S. Tinkloh, T. Wu, T. Tröster, T. Niendorf, A micromechanical-based finite element simulation of process-induced residual stresses in metal-CFRP-hybrid structures, Compos. Struct. 238 (2020) 111926, doi:10.1016/j.compstruct.2020.111926.

[10] A.A. Hanson, S.M. Nelson, A.J. Skulborstad, B.T. Werner, T.M. Briggs, Simulating residual stresses in simple multi-material composite structures, in: Proceedings of the CAMX 2017 Composites and Advanced Materials Expo, vol. 2017 December, 2017.

[11] A. Ding, S. Li, J. Wang, L. Zu, A three-dimensional thermo-viscoelastic analysis of process-induced residual stress in composite laminates, Compos. Struct. 129 (2015) 60–69, doi:10.1016/j.compstruct.2015.03.034.

[12] R. Prussak, D. Stefaniak, E. Kappel, C. Hühne, M. Sinapius, Smart cure cycles for fiber metal laminates using embedded fiber Bragg grating sensors, Compos. Struct. 213 (2019) 252–260, doi:10.1016/j.compstruct.2019.01.079.

[13] P.P. Krimbalis, C. Poon, Z. Fawaz, K. Behdinan, On the prediction of induced residual stresses in fibre metal laminates, in: Design, Manufacturing and Applications of Composites: Proceedings of the 7th Joint Canada-Japan Workshop on Composites, 2008, pp. 125–132.

[14] C. Bellini, W. Polini, L. Sorrentino, A new class of thin composite parts for small batch productions, Adv. Compos. Lett. 23 (2014) 115–120.

[15] Z. Yuan, G. Yang, Z. Yang, A. Tang, S. Li, Y. Li, Effect of metal–fiber shear interaction on curing deformation of fiber metal laminates, Arab. J. Sci. Eng. 45 (2020) 5375–5384, doi:10.1007/s13369-020-04438-1.

[16] L. Che, G. Fang, Z. Wu, Y. Ma, J. Zhang, Z. Zhou, Investigation of curing deformation behavior of curved fiber metal laminates, Compos. Struct. 232 (2020), doi:10.1016/j.compstruct.2019.111570.

[17] L. Sorrentino, C. Bellini, L. Carrino, A. Leone, E. Mostarda, L. Tersigni, Cure process design to manufacture composite components with variable thickness by a closed die technology, in: Proceedings of the 17th International Conference on Composite Materials, Edinburgh, 2009.

[18] S. Shevtsov, I. Zhilyaev, A. Soloviev, I. Parinov, V. Dubrov, Optimization of the composite cure process based on the thermo-kinetic model, Adv. Mater. Res. 569 (2012) 185–192, doi:10.4028/www.scientific.net/AMR.569.185.

[19] L. Sorrentino, C. Bellini, Validation of a methodology for cure process optimization of thick composite laminates, Polym. Plast. Technol. Eng. 54 (2015) 1803–1811, doi:10.1080/03602559.2015.1050513.

[20] H. Rydarowski, M. Koziol, Repeatability of glass fiber reinforced polymer laminate panels manufactured by hand lay-up and vacuum-assisted resin infusion, J. Compos. Mater. 49 (2015) 573–586, doi:10.1177/0021998314521259.